Interlibrary Loans, Carleton University Library

QMUQS

Universite du Quebec a Montreal, Bibliotheque des sciences
Pret entre bibliotheques
C.P. 8889, Succursale Centre-ville
Montreal, QC   H3C 3P3
Canada

ATTN:		SUBMITTED:	2016-04-20
PHONE:	514-987-3000	PRINTED:	2016-04-20 09:30:00
FAX:	514-987-6821	REQUEST NO.:	REG-10054855
E-MAIL:	PEB_QMUQS@UQUEBEC.CA	SENT VIA:	Manual
		EXTERNAL NO.:	RSP#8581373

REG   Regular   **Copy**   **Journal**

NOTES: jl: 20-04-16. Sent 1 article.

REQUESTER INFO: RQ#1761481
DELIVERY: Ariel: 132.208.68.254
REPLY: E-mail: PEB_QMUQS@UQUEBEC.CA

For OOCC Queries: contact Interlibrary Loans at 613-520-2732

or email at: raceradm@library.carleton.ca

Low Density of Gold Nanorods in the Anodic Layer for Enhancing the Efficiency of Organic Solar Cells

Alaa Y Mahmoud[1], Jianming Zhang[2], Jayanta K Baral[1,3], Ricardo Izquierdo[3], Dongling Ma[2], Muthukumaran Packirisamy[4] and Vo-Van Truong[1]

[1]Department of Physics, Concordia University, Montréal, Québec, Canada H4B 1R6
[2]Énergie, Matériaux et Télécommunications, Institut National de la Recherche Scientifique ,1650 Boulevard Lionel-Boulet, Varennes, Québec, Canada J3X 1S2,
[3]Département d'informatique, Université du Québec à Montréal, Montréal, Québec, Canada H3C 3P8
[4]Department of Mechanical Engineering, Concordia University, Montréal, Québec, Canada H3G 1M8

ABSTRACT

The effect of using an anodic layer with low density ($\sim 6 \times 10^8$ cm^{-2}) of gold nanorods (GNR) in organic bulk heterojunction poly(3-hexylthiophene) (P3HT) and phenyl-C$_{61}$-butyric acid methyl ester (PCBM) solar cells was studied. GNRs were deposited using several techniques, which produced various densities of GNRs on the anode layer. The anodic layers were characterized microscopically and spectroscopically. The power conversion efficiency and the short-circuit current for experimental devices incorporating GNR anodic layer showed an enhancement of up to 18% as compared to the control device. The results suggest that the electric field in the P3HT:PCBM active layer was increased by the localized surface plasmon resonances in GNRs. The increase in the electric field enhanced the photo-generation of excitons in the active layer near the plasmon peak, which improved the short-circuit current and the overall power conversion efficiency. Interestingly, photovoltaic devices with a low density of GNRs in the anodic layer showed an increase in the power conversion efficiency that was superior to that of devices with a higher density of GNRs in the anodic layer. This suggests that although the anodic layer with a higher density of GNRs absorbed more light, part of this light was confined in the anodic layer itself, and prevented from reaching the active layer of the bulk heterojunction device. In such cases, the power conversion efficiency was even found to be decreased with respect to the value for the control device.

Organic bulk heterojunction, solar cell, gold nanorods, surface plasmon resonance, anodic layer.

1. INTRODUCTION

Converting the solar radiation into electricity via organic solar cell (OSC) has recently attracted a great deal of solar energy researchers interest. Among the different types of solar cells, the exceptional features of OSCs such as flexibility, ease of processing, portability, and low cost of production make them most interesting for producing energy from light[1-2]. So far, the highest reported efficient value of polymer/fullerene OSCs was made from a poly (3-hexylthiophene-2,5-diyl) (P3HT) polymer as a donor, and a phenyl-C$_{61}$-butyric acid methyl ester (PCBM) fullerene-derivative as an acceptor is up to 5%[2-3].

Efficient absorption of the solar radiation is a desirable goal to achieve a high-performance photovoltaic (PV) device. The high value of the absorption coefficient for OSCs ($>10^5$ cm^{-1}) allows a very thin active layer ($\sim$100 nm) to absorb a reasonable amount of the incident radiation[1]. However, due to the short diffusion length of excitons[1-2] ($\sim$10-20 nm) the thickness of OSCs, or more specifically the thickness of the active layer (polymer/fullerene layer), has to be

limited. If the thickness of the active layer is decreased, the amount of the absorbed light by the active layer is reduced and the total power conversion efficiency (PCE) can be as well[2].

The introduction of the bulk heterojunction (BHJ) concept[4-5], allowing for the use of thicker active layer films, succeeded to achieve more efficient OSC devices by reducing the distance between donor/acceptor interface, which facilates the dissociation of excitons and enhances the PV performance. Although a thick active layer would absorb more light, a noticeable drop in the PCE was observed in this case[6-7]. This was due to the increase in the device series resistance making the surface recombination of charge carriers becoming significant[7].

Alternatively, it has been reported that inserting metallic nanoparticles (MNP) into OSC layers enhanced the light harvesting without increasing the thickness of the active layer [6]. The plasmonic effect in MNPs helped to concentrate more light on the active layer, thus to increase the absorption. Localized surface plasmon resonance (LSPR) in MNPs is a phenomenon of collective oscillations of conduction electrons upon light illumination, which enables more light absorption in the visible region of the spectrum. It has been reported that the PCE of OSCs increased by a factor of about 1.5 by incorporating silver and gold MNPs into the PV device layers [3][6][8-10].

To our knowledge, there have been no previous inquiries on the impact of gold nanorods (GNRs) on the performance of OSCs. Hence in this study, the effect of depositing a GNRs layer on the top of OSC anodic electrode by simple coating methods such as spin-casting, drop-casting, and vertical deposition technique was investigated. A comparison between the efficiency of resulting devices was made.

2. EXPERIMENTAL DETAILS

2.1 Gold Nanorods

2.1.1 Chemicals and Materials

Hydrogen tetrachloroauric acid ($HAuCl_4 \cdot 3H_2O$), cetyltrimethylammonium bromide (CTAB), sodium borohydride ($NaBH_4$), silver nitrate ($AgNO_3$) and ascorbic acid (AA) were purchased from Sigma-Aldrich. Ultrapure deionized (DI) water (Millipore system) was used throughout the experiments.

2.1.2 Gold nanorods preparation[11]

a. Seed Solution: CTAB solution (2.5 ml, 0.2 M) was mixed with 1.5 ml of 1 mM $HAuCl_4 \cdot 3H_2O$ and stirred for a while. Afterwards, 0.6 ml of ice-cold 0.01 M $NaBH_4$ was added to the stirred solution. As a result, a brownish-yellow seed solution is formed. Vigorous stirring of the seed solution was continued for 2 min. The solution was kept at 25°C after stirring.

b. Growth solution: The growth solution was prepared by mixing all the following components: 10 ml of 0.2 M CTAB, 560 μl of 4 mM $AgNO_3$, 1 ml of 15 mM $HAuCl_4 \cdot 3H_2O$ and 9 ml of DI water. Approximately 250 μl of AA (0.08 M) was slowly added to the mixture. The addition of ascorbic acid was conducted drop-wise; until the mixture became colourless after adding one quarter more of the total number of droplets to that point.

c. Nanorods colloidal solution: The final step was the addition of 200 μl of the seed solution to the growth solution at 27-30°C. The colour of the resulted solution gradually changed into brownish-red within 10-20 min. The temperature of the growth medium was kept constant at 27-30°C during the full procedure.

The concentration of GNRs in the aqueous solution was calculated to be ~1.593×10^{12} rods/mL, while the average aspect ratio was ~ 4 as it was revealed by transmission electron microscopy (TEM) (Fig. 1a). Fig. 1b shows the UV-Vis spectrum for the GNR colloidal solution. The absorption maxima for both longitudinal and transverse modes were 715

nm and 520 nm respectively. The two absorption modes originated from the excitation of conduction electrons respectively in the directions parallel and perpendicular to the rod long axis[11].
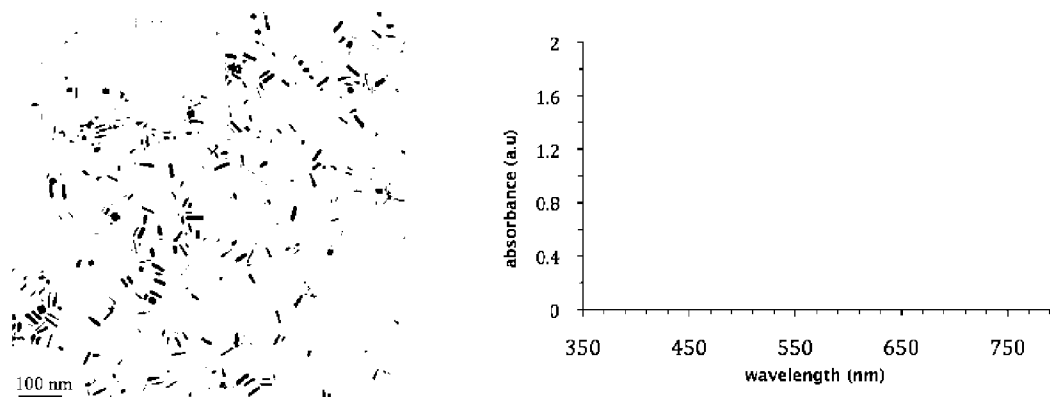

Fig. 1. (a) TEM image showing GNRs on glass. (b) UV-Vis spectra corresponding to the GNRs colloidal solution showing the absorption maxima at 715 nm and 520 nm for longitudinal mode and transverse mode respectively.

2.2 Organic Solar Cells

2.2.1 Chemicals and Materials

Poly(3,4-ethylenedioxythiophene) poly(styrenesulfonate) (PEDOT:PSS) (CLEVIOS™ P VP AI 4083) was purchased from HC Stark. P3HT with a high regioregularity (98%) and an average molecular weight of <50,000 MW was purchased from Rieke Metals. PCBM (>99.5%) and 1, 2-dichlorobenzene (anhydrous, 99%) were purchased from Sigma-Aldrich. Aluminium (Al) wire and lithium fluoride (LiF) were purchased from Alfa Aesar. The materials were used as received without further purification.

2.2.2 Device Fabrication[12]

A polymer bulk heterojunction solar cell is an active layer that is placed in-between two electrodes, a transparent positive anode and a negative metallic cathode.

a. Anode materials and treatment: Patterned indium tin oxide (ITO)-coated glass substrates (2.6 cm × 3.7 cm) were cleaned with detergent, rinsed with DI water, and then successively ultrasonicated in acetone, isopropanol and DI water for 20 min each. The substrates were then dried with a nitrogen flow and baked at 150°C for 20 min. Prior to PEDOT:PSS deposition, the substrates were subjected to an oxygen plasma treatment for 35s. PEDOT:PSS then was passed through a 0.45 μm PVDF membrane filter and spun-cast on the top of ITO-coated glass under an ambient environment. To be dehydrated, the substrates were baked at 120°C for 1h and afterwards, the substrates were transferred to a nitrogen glove box in which the active layer deposition took place.

b. Active layer: In a nitrogen glove box environment with a pressure of 3 mbar and a humidity level less than 0.1 ppm, a blend of P3HT:PCBM with a ratio of 1:0.8, and a concentration of 20 mg/ml (P3HT) was dissolved in 1, 2-dichlorobenzene, passed through a 0.45 μm PTFE membrane filter and then spun-cast at 1000 rpm on the top of the ITO/PEDOT:PSS modified anode. The substrates were then left to dry in covered Petri dishes for 30 min before they were transferred to the evaporator system.

c. Cathode materials and deposition: To finalize the device, a bilayer cathode was thermally evaporated through a shadow mask under a pressure inferior to 10^{-5} torr. The cathode materials were LiF (~1nm) and Al (~90 nm) and the

evaporation rates were ~1 A/s and ~2.5-5 A/s for LiF and Al respectively. The material thicknesses were determined with a mechanical profilometer (Veeco Dektak150).

  d. Annealing: Post-production annealing was performed inside the glove box in which the devices were placed in direct contact with a digital hotplate. The annealing was performed at 160°C for 30 min. The devices were then left to cool-down before characterization.

  e. Gold nanorod layer: after oxygen plasma treatment of the ITO-coated substrates, the GNRs were deposited on the top of ITO before spin-casting PEDOT:PSS. Three different deposition approaches were used: drop-casting, spin-casting and vertical deposition technique. For drop-casting, the substrates were covered with drops of GNR colloidal solution then placed in a microwave for 8 min. Spin-casting was performed with two steps, 200 rpm for 3s then 1000 rpm for 10s. For vertical deposition, the substrates were placed vertically in the GNR colloidal solution (Fig. 2a) for different periods of time.

  Each substrate includes 8 devices (Fig. 2b), with an active area, that is the area between the ITO and the Al layers, of 0.16 cm^2. Both control (without GNR) and experimental (with GNR) devices were fabricated and tested during the same batch of process. The control and experimental devices had respectively the following configurations: ITO/PEDOT:PSS/P3HT:PCBM/LiF/Al and ITO/GNR/PEDOT:PSS/P3HT:PCBM/LiF/Al (Fig. 2c).
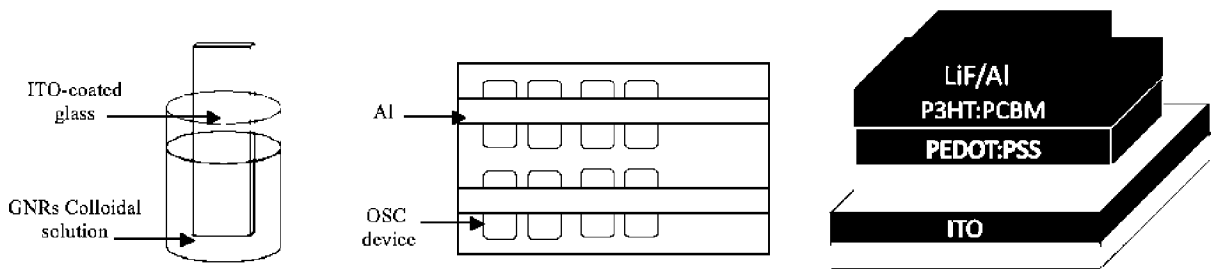

Fig. 2. (a) Vertical deposition of GNRs on ITO-coated glass. (b) Schematic diagram showing the position of 8 OSC devices on ITO-coated glass substrate. (c) Schematic structure for BHJ OSC showing the position of GNR anodic layer in the PV device.

2.2.3   Device Characterization

  Devices were tested under ambient conditions without any device encapsulation. The devices were placed beneath solar simulator made of a xenon lamp (Oriel instruments) that was equipped with AM 1.5G filter. The output intensity of the lamp was adjusted to 100 mW/cm^2 using an LI-250 light meter (Bioscience). The current-voltage measurements were carried out using a source meter (Keithley 2400).

2.2.4   Experimental Procedures

  GNRs layers were deposited on the top of ITO-coated glass with three different methods, namely drop-casting, spin-casting and vertical deposition, and the optical absorbances and particle densities of the resulted layers were compared. In a second experiment, comparison was made between a set of samples with single and multilayers (5-layers) of GNRs that were deposited by spin-casting. Finally, a comparison was between samples made using various periods of vertical deposition (10, 30 and 50 min). For all the previous sets of samples, the optical absorption of the GNR layers was measured using a UV-Vis spectrophotometer (PerkinElmer LAMBDA 650 spectrophotometer) and the surface structure was characterized using a scanning electron microscopy (FEG-SEM Hitachi S-4700).The GNR densities in the anodic layer were determined using the electron micrographs.

Solar cells were fabricated with various conditions of GNR deposition, and the PV parameters such as the open-circuit voltage (V_{oc}), the short-circuit current (J_{sc}), the fill factor (FF) and the PCE were measured in devices with and without GNRs, under the same experimental conditions.

3. RESULTS AND DISCUSSION

By varying the deposition techniques, GNRs with different densities and alignments were produced on the top of ITO-coated glass as it is demonstrated by SEM images in Fig. 3. The spectral measurements (Fig.4a) of the obtained GNRs layers show a noticeable difference in the plasmonic absorption peaks; the drop-casted particles shows two peaks, while a shoulder and a peak are found in the case of particles obtained by the vertical deposition method. A more intense peak is observed for the spin-casted deposit. As shown in Fig. 3a, drop-casted and 5-layers spin-casted (not presented) GNRs produced denser rods in the anodic layer ($\sim 4 \times 10^9$ cm^{-2}) with nanorod long-axis alignments parallel and perpendicular to the substrate plane. The presence of GNRs with the two different alignments at the surface explains the appearance of the two peaks in the spectrum. For one-layer spin-casted rods, the rod long-axis alignment was mostly in the substrate plane (Fig. 3b), which supports the longitudinal resonance peak in the spectrum of figure 4a. In the case of vertically deposited rods (Fig. 3c), additionally to the longitudinal resonance peak there is the transverse resonance mode, which indicates that some particles were aligned perpendicularly to the substrate plane. For vertically deposited and one-layer spin-casted rods, the particles densities on the anodic layer were evaluated from SEM images to be $\sim 6 \times 10^8$ cm^{-2} and $\sim 8 \times 10^8$ cm^{-2} respectively.
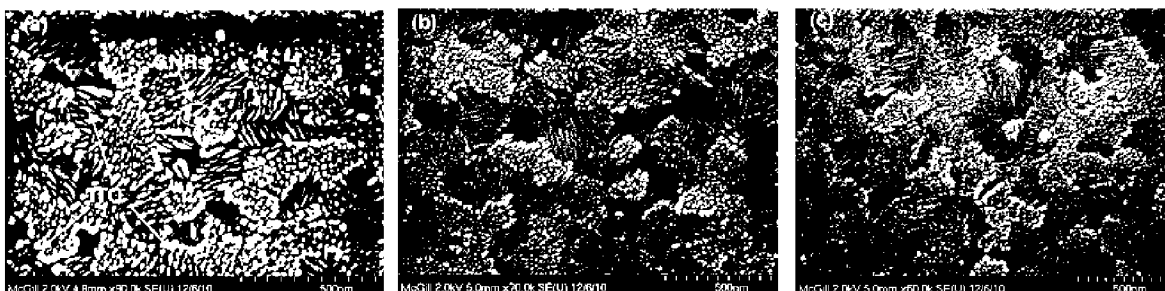

Fig. 3. SEM images for GNRs deposited on ITO-coated glass using different methods (a) drop-casting, (b) spin-casting and (c) vertical deposition.
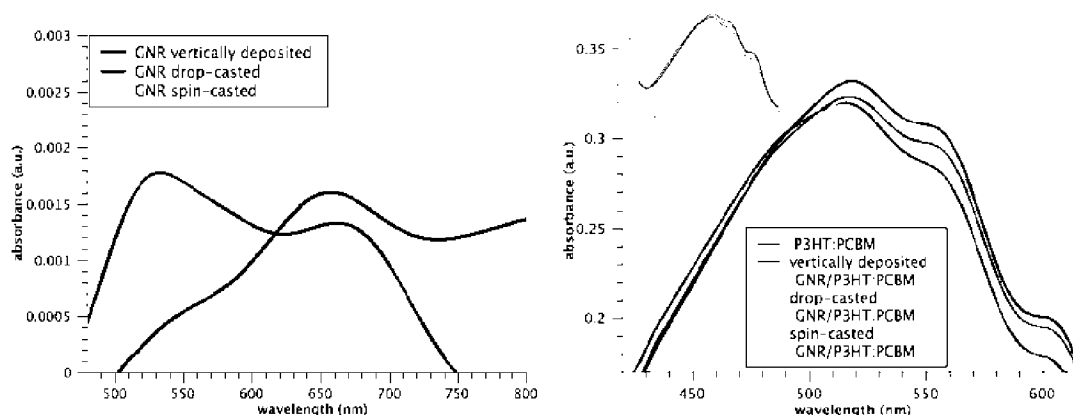

Fig. 4. (a) UV-Vis spectra for GNRs deposited on ITO-coated glass with various deposition techniques. (b) A comparison between the optical density of P3HT:PCBM with and without GNRs on the ITO-coated glass. The inset shows the absorption profile for P3HT:PCBM from 380 nm to 660 nm with and without GNRs.

Fig. 4b shows the optical density of the active layer (P3HT:PCBM) on ITO-coated glass with and without incorporating the GNR plasmonic layer. Due to the match between the optical absorption of both plasmonic (500-700 nm) and P3HT:PCBM (380-660 nm), the addition of GNRs increased the optical density for the active layer up to ~11%, and the resulting absorption profile for GNRs/P3HT:PCBM was the same as that for the pristine one (inset of Fig.4b).
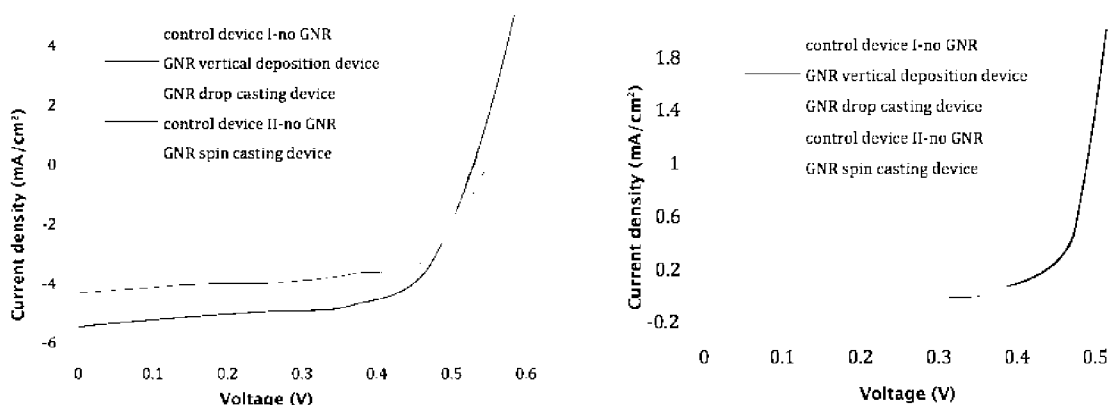

Fig. 5. IV curves for both control (ITO/P3HT:PCBM/LiF/Al) and experimental (ITO/GNRs/P3HT:PCBM/LiF/Al) devices (a) under illumination. (b) in darkness.

Fig. 5 shows the IV characteristics for solar cells made with and without GNR anodic layers under solar simulator illumination (5a) and in the darkness (5b). The PV parameters for those devices are summarized in Table 1. From this table, we can observe that the addition of the plasmonic layer increased the J_{sc} for the OSC device in most cases, which in turn increased the PCE. This is in accordance with previously reported results for gold nanoparticles[6][8][10]. The enhancement in the PCE was 5% and 15% for one layer of GNRs that was deposited using spin-casting and vertical deposition approaches respectively. Nevertheless, solar cells having higher density of GNRs, ~ 4×10^9 cm^{-2}, deposited either by drop-casting or by spin-casting of 5-layers of GNRs on the top of ITO-coated glass showed a slightly lower performance than control devices without GNRs. In these cases, the efficiency was decreased by up to 2%.

Device type	GNR density (cm^{-2})	V_{oc}(V)	J_{sc}(mA/cm^2)	V_{max} (V)	FF %	PCE %	Enhancement
Control device I	-	0.4737	-4.7122	0.3684	67.95	1.5168	
Vertically deposited GNR	~6 × 10^8	0.4737	-5.3809	0.3684	69.01	1.759	+16%
Drop-casted GNR	~4 × 10^9	0.4737	-4.8284	0.3684	64.88	1.4839	-2%
Control device II	-	0.5385	-4.2091	0.4359	68.28	1.5475	
Spin casted GNR-1 layer	~8 × 10^8	0.5385	-4.5055	0.4359	66.89	1.6226	+5%
Spin casted GNR- 5 layers	~4 × 10^9	0.5897	-4.1069	0.4872	63.43	1.5364	-0.8%

Table 1. The PV parameters for control devices (without GNR) and experimental one (with GNR) at the incident power intensity of 100 mW/cm^2 under AM 1.5G filtered spectral illumination for different deposition methods.

The increase in the efficiency of solar cells with the GNRs anodic layer could be explained as follows. Localized surface plasmon resonance in GNRs acts as a light antenna[10], increasing the local electric field around GNRs, which in turn increase the light absorption in the surrounding area. Due to its proximity to the GNR anodic layer, the increase in the light absorption takes place mostly in the active layer. This enhanced absorption increases the photo-generation of excitons in the active layer near the plasmon peak, which enlarges the J_{sc} and improves the PCE in general.

The decrease in the device efficiency via increasing GNRs density in the anodic layer in the case of drop-casting and 5-layers spin-casting could be due to the surface recombination of charge carriers at the interface between the anodic and the active layers[13], or due to the 'hot-spots' that were generated from the dipole-dipole interaction of the randomly distributed dense GNRs in the anodic layer. In such case, a hybridized plasmonic state was generated, which disturbed the electromagnetic profile in the active layer and affected the excitons-plasmons interaction. Hence, a drop in the PCE was observed[8].

As we found, GNR layers that produced by the vertical deposition method increased significantly the PCE of solar cells. Hence, we tried to maximize this effect by studying some deposition parameters, such as depositing time, in this process. To study the effect of varying time on the vertical deposition method, rods were deposited respectively at 10, 30 and 50 min. The SEM images in Fig. 6 show that a 50 min deposition period produced more particles ($\sim 8 \times 10^8$ cm^{-2}) as compared to 10 and 30 min deposition periods where the particle density was observed to be $\sim 6 \times 10^8$ cm^{-2}. The variation in the deposition time affected the absorption of the resulting layer too as demonstrated in Fig. 7a.
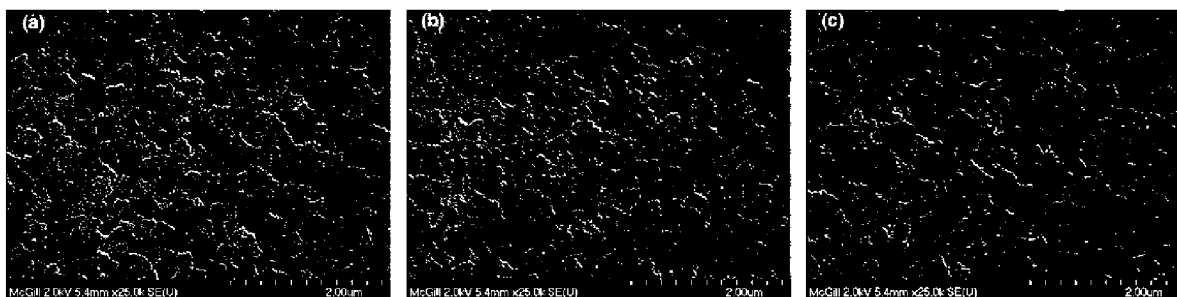

Fig. 6. SEM images for GNRs deposited on ITO-coated glass using the vertical deposition method with different deposition times (a) 10 min, (b) 30 min and (c) 50 min.
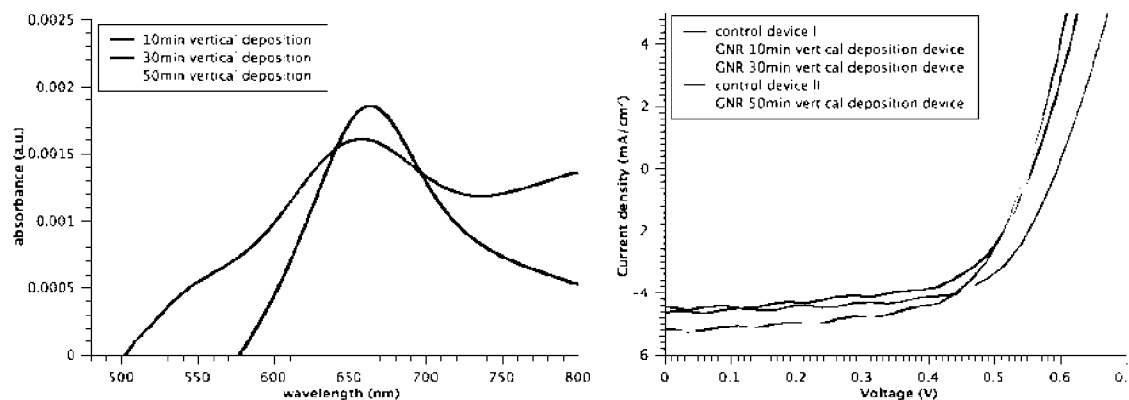

Fig. 7. (a) UV-Vis spectra for GNRs deposited on ITO-coated glass with various vertical deposition periods. (b) IV curves for both control (ITO/P3HT:PCBM/LiF/Al) and experimental (ITO/GNRs/P3HT:PCBM/LiF/Al) devices under AM 1.5G spectral illumination. The deposition times were 10, 30, and 50 min.

Fig. 7b shows the influence of the deposition time on the IV characteristics of the solar cells made with those layers, and Table 2 summarizes the obtained PV parameters. Among the 10, 30 and 50 min deposition periods, the 30 min vertically deposited GNRs produced the highest (18%) enhancement in the PCE, from 1.58 % to 1.85 %. This increase of the efficiency is due to a 16% enhancement (from -4.48 to -5.24 mA/cm^2) in the J_{sc}.

Device type	GNR density (cm^{-2})	V_{oc}(V)	J_{sc}(mA/cm^2)	V_{max} (V)	FF %	PCE %	Enhancement
Control device I	-	0.5656	-4.4847	0.4141	62.39	1.5826	
10 min vertical deposition	$\sim 6 \times 10^8$	0.5909	-4.5951	0.4394	65.78	1.7862	+13%
30 min vertical deposition	$\sim 6 \times 10^8$	0.5656	-5.2453	0.4141	62.39	1.8510	+18%
Control device II	-	0.5404	-5.0333	0.4141	64.29	1.7486	
50 min vertical deposition	$\sim 8 \times 10^8$	0.5404	-5.2364	0.4394	65.23	1.8458	+3%

Table 2. The PV parameters for pristine control devices and devices in the presence of GNRs at the incident power intensity of 100 mW/cm^2 under AM 1.5G filtered spectral illumination for different GNR vertical deposition times.

In this study, the PV parameters were determined at ±5 % error and the superior enhancement in the PCE due to 30 min vertical deposition of GNRs was reproducible. Yet, those results cannot be fully generalized as it depends very much on the concentration of GNRs in the colloidal solution. However, a general trend for the increase of PCE of organic solar cells can be envisioned. In addition, further investigations have to be done to study the effect of the surface treatment of the ITO-coated glass on the GNRs deposition.

4.   CONCLUSION

This study demonstrates the influence on the PV performance of both density and alignment of GNRs that were deposited on the anodic layer of an organic solar cell by three simple methods, namely the drop-casting, spin-coating and vertical deposition. Due to the plasmonic effect, GNRs with density $\sim 6 \times 10^8$ cm^{-2} produced by 30 min vertical deposition enhanced the PCE by up to 18%. The presence of localized surface plasmon resonances in GNRs would enhance the electric field in the active layer, which in turn improved the photo-generation of excitons in the bulk heterojunction blend, leading to a more efficient generation of charge carriers that increased the J_{sc} by up to 16%. However, the results also suggest that a higher density of GNRs does not necessarily lead to improvements in the overall efficiency in all cases.

5.   ACKNOWLEDGEMENTS

6.   BIBLIOGRAPHY

[1]   Gunes, S., Neugebauer, H., Sariciftci, N. S., "Conjugated polymer-based organic solar cells", Chem. Rev., 107(4), 1324–1338 (2007).

[2] Li, L. G., Lu, G. H., Yang, X. N., Zhou E. L., "Progress in polymer solar cell", Chinese Sci. Bull., 52(2), 145-158 (2007).

[3] Kim, S. S., Na, S. I., Jo, J., Kim, D. Y., Nah, Y. C., "Plasmon enhanced performance of organic solar cells using electrodeposited Ag nanoparticles", Appl. Phys. Lett., 93(7), 073307 (2008).

[4] Yu, G., Gao, J., Hummelen, J. C., Wudl, F., Heeger, A. J., "Polymer Photovoltaic Cells: Enhanced Efficiencies via a Network of Internal Donor-Acceptor Heterojunctions", Sci. 270(5243), 1789-1791(1995).

[5] Shaheen, S. E., Brabec, C. J., Sariciftci, N. S., Padinger, F., Fromherz, T., Hummelen, J. C., "2.5% efficient organic plastic solar cells ", Appl. Phys. Lett. 78(6), 841 (2001)

[6] Shen, H., Bienstman, P., Maes, B., "Plasmonic absorption enhancement in organic solar cells with thin active layers", J. Appl. Phys., 106(7), 073109 (2009).

[7] Moliton, A., Nunz, J-M., "How to model the behaviour of organic photovoltaic cells", Polym. Int. 55(6), 583–600 (2006).

[8] Lee, J. H., Park, J. H., Kim, J. S., Lee, D. Y., Cho, K., "High efficiency polymer solar cells with wet deposited plasmonic gold nanodots", Org. Electron., 10(3), 416-420 (2009).

[9] Morfa, A. J., Rowlen, K. L., "Plasmon-enhanced solar energy conversion in organic bulk heterojunction photovoltaics", Appl. Phys. Lett., 92(1), 013504 (2008).

[10] Atwater, H. A., Polman, A., "Plasmonic for improved photovoltaic devices", Nat. Mater., 9(3), 205-213 (2010).

[11] Sau, T. K., Murphy, C. J., "Seeded high yield synthesis of short Au nanorods in aqueous solution", Langmuir, 20(15), 6414-6420 (2004).

[12] Li, G., Shrotriya, V., Huang, J., Yao, Y., Moriarty, T., Emery, K., Yang, Y., "High-efficiency solution processable polymer photovoltaic cells by self-organization of polymer blends", Nat. Mater., 4(11), 864-868 (2005).

[13] Yoon, W-J., Jung, K-Y., Liu, J., Duraisamy, T., Revur, R., Teixeira, F. L., Sengupta, S., Berger, P. R., "Plasmon-enhanced optical absorption and photocurrent in organic bulk heterojunction photovoltaic devices using self-assembled layer of silver nanoparticles", Sol. Energy. Mater. Sol. Cells, 94(2), 128-132 (2009).